Global Intraurban Intake Fractions for Primary Air Pollutants from Vehicles and Other Distributed Sources

Joshua S. Apte,[†] Emilie Bombrun,[‡] Julian D. Marshall,*,[‡] and William W. Nazaroff[§]

[†]Energy and Resources Group, University of California, Berkeley, California 94720-3050, United States
[‡]Department of Civil Engineering, University of Minnesota, Minneapolis, Minnesota 55455-0233, United States
[§]Department of Civil and Environmental Engineering, University of California, Berkeley, California 94720-1710, United States

S *Supporting Information*

ABSTRACT: We model intraurban intake fraction (iF) values for distributed ground-level emissions in all 3646 global cities with more than 100 000 inhabitants, encompassing a total population of 2.0 billion. For conserved primary pollutants, population-weighted median, mean, and interquartile range iF values are 26, 39, and 14−52 ppm, respectively, where 1 ppm signifies 1 g inhaled/t emitted. The global mean urban iF reported here is roughly twice as large as previous estimates for cities in the United States and Europe. Intake fractions vary among cities owing to differences in population size, population density, and meteorology. Sorting by size, population-weighted mean iF values are 65, 35, and 15 ppm, respectively, for cities with populations larger than 3, 0.6−3, and 0.1−0.6 million. The 20 worldwide megacities (each >10 million people) have a population-weighted mean iF of 83 ppm. Mean intraurban iF values are greatest in Asia and lowest in land-rich high-income regions. Country-average iF values vary by a factor of 3 among the 10 nations with the largest urban populations.

1. INTRODUCTION

Air pollution exposure is associated with adverse health effects.[1−4] Efforts to improve air quality focus on reducing emissions. Air quality management includes deciding which sources to control and by how much. Intake fraction estimates could help guide such prioritization efforts.

Intake fraction (iF) summarizes the emission-to-intake relationship for a specific source as the fraction of emissions that are inhaled by an exposed population.[5] Intake fraction can be used in cost-benefit and cost-effectiveness analyses, investigations of environmental equity, health risk assessment, and other studies that estimate the exposure consequences of emissions.[6−8]

Intake fraction varies spatially and temporally, depending on factors such as the size of the exposed population, proximity between people and emissions, and environmental persistence of a pollutant. Reported iF values for nonreactive motor vehicle emissions include the following results: 0.1−0.5 ppm for U.S. rural areas,[9] 3−21 ppm for U.S. cities of typical size,[10,11] and 29−280 ppm for three global megacities (Los Angeles,[12] Mexico City,[13] and Hong Kong[14]). An iF of 10 ppm (i.e., 10^{-5}) means that an exposed population inhales an aggregate increment of 10 grams per tonne emitted. Prior investigations of iF for urban vehicle emissions have emphasized conditions for North America and Europe; determinants such as meteorology and urban form may differ on other continents. Moreover, vehicle use is increasing rapidly in countries such as China and India for which few iF estimates exist.[15−19]

Here, we use a modeling approach to estimate intraurban iF values for distributed ground-level primary pollutant emissions for all worldwide cities with a year 2000 population of 100 000 or more. In aggregate, this set of 3646 cities contains 2.0 billion people (for year 2000), including ~1 billion people in Asia. A goal of this study is to elucidate global patterns of intraurban iF among countries, regions, and cities of varying sizes. We extend a previously published approach for estimating iF,[13] incorporating global data sets of demographic and meteorological parameters as model inputs. Our investigation is motivated by trying to better understand the exposure consequences of urban vehicle emissions. The results may be informative for any broadly distributed source of ground-level emissions to outdoor urban air.

2. METHODS

2.1. Intake Fraction. The intake fraction for atmospheric emissions can be evaluated as

$$\text{intake fraction} = \frac{\text{population intake}}{\text{total emissions}}$$

$$= \frac{\int_{T_1}^{\infty} \left(\sum_{i=1}^{P} (C_i(t) Q_i(t)) \right) dt}{\int_{T_1}^{T_2} E(t) dt} \quad (1)$$

where T_1 and T_2 are the starting and ending times of emissions, P is the number of people exposed, $Q_i(t)$ is the volumetric breathing rate ($m^3 \, s^{-1}$) for individual i at time t, $C_i(t)$ is the incremental concentration ($g \, m^{-3}$) at time t in individual i's breathing zone that is attributable to the emissions, and $E(t)$ is the emission rate ($g \, s^{-1}$) at time t.[12] The integrals in eq 1 are evaluated numerically, as detailed below.

2.2. Emissions−Exposure Concentration Relationship. *2.2.1. Model Selection.* Intake fractions depend on the relationship between emissions and exposure concentrations. Previous studies have employed various methods with differing levels of complexity and data requirements. Examples include one-compartment Eulerian models,[8,10,11] Gaussian plume models,[20,21] coarse-grid Eulerian models,[13,22] empirical estimates using tracers of opportunity,[12,13,23,24] and intentional tracer-gas experiments.[25]

In this paper, we designate urban areas with a population of at least 100 000 as "cities". For the large number of cities considered here, an efficient approach is needed that can provide good estimates with a reasonable level of effort per city. We consider spatially distributed ground-level emissions sources (e.g., vehicles) and use a one-compartment Eulerian model. We estimate the intraurban iF for each city, i.e., the iF associated with residents' inhalation of emissions from their city.

Compared to alternatives, there are several advantages of the one-compartment Eulerian model: (1) Input data are available globally using uniform methods. (2) Studies comparing iF estimated using this model have found similar results compared with studies using empirical data or complex air-dispersion models.[11,12] (3) Because this type of model is widely used,[26−28] the results reported here can be directly applied as model input parameters. (4) The one-compartment model is readily scaled in size for each location studied. Among the limitations of this approach are that (1) the model excludes within-urban variability, (2) we have not evaluated iF for secondary pollutants or for nonconserved species with other than first-order decay, and (3) as applied here, we only consider intraurban exposures. Previous findings suggest that for estimating iF for individual cities, this approach is accurate within a factor of ∼2 or better for primary pollutants.[11−13] We judge this accuracy to be acceptable given the efficiency of the approach; global intraurban iF values reported here vary by much more than a factor of 2.

2.2.2. One-Compartment Emissions−Concentration Model. The following equation, derived from mass balance, embodies a dynamic one-compartment model for predicting a primary-pollutant concentration increment resulting from emissions:[13,29]

$$\frac{dC(t)}{dt} = \frac{E(t)}{LWH(t)} - C(t)\left(k + \frac{u(t)}{L} + \phi \frac{1}{H(t)} \frac{dH}{dt} \right) \quad (2)$$

Here, $C(t)$ is the incremental concentration attributable to the emissions source ($g \, m^{-3}$), which varies with time, t (s), $E(t)$ is

the emission rate from the source under consideration ($g \, s^{-1}$), L and W are the windward and crosswind dimensions, respectively (m), of the model domain, $H(t)$ is the atmospheric mixing height (m), k is the first-order decay constant (s^{-1}), and $u(t)$ is the wind speed averaged over the mixing height ($m \, s^{-1}$). The parameter ϕ accounts for dilution of contaminated urban air by clean air aloft during periods of increasing mixing height as follows: $\phi = 0$ when dH/dt is nonpositive (H decreasing or constant), and $\phi = 1$ when dH/dt is positive (H increasing). Stevens et al.[13] were the first to apply this dynamic model to estimate urban iF; eq 2 extends their approach to incorporate pollutants that undergo first-order decay with rate constant k. Base-case iF analyses are presented in this paper for conserved, nonreactive emissions ($k = 0$). Many important vehicle-emitted species—such as carbon monoxide (CO), benzene, and primary (i.e., directly emitted) constituents of fine particulate matter ($PM_{2.5}$), including black carbon particles—are reasonably modeled as conserved within urban areas, since $k \ll u/L$. Sensitivity cases are simulated for decaying pollutants with 10 and 100 h half-lives ($k = 1.7$ and $0.17 \, d^{-1}$, respectively). Example species in these classes are acetaldehyde and toluene (∼10 h half-life) and methyl *tert*-butyl ether (MTBE; ∼100 h half-life).[30] For the primary pollutants considered here, the iF is independent of the time-averaged emissions rate.[6] Likewise, the intraurban primary-pollutant iF for any source is, by definition, independent of background concentrations imposed by other sources and by regional transport. Consequently, city-specific emissions and concentration data are not required as model inputs.

In implementation, eq 2 is converted from differential to finite-difference form, and the model simulates a series of time steps. We use short time steps: 7.5 min for a 3 year simulation of each urban area. We assumed a constant annual-average emission rate for all cities in our data set and specified initial and upwind boundary conditions for each city as $C = 0$. We tested the numerical integration to ensure it behaves as expected for these conditions: (1) in simple scenarios with known outcome (e.g., step change for one input parameter) and (2) by matching inputs and outputs from Stevens et al.[13] Discretization errors resulting from numerical integration of eq 2 are estimated to be less than 1%.

2.3. Model Input Data. *2.3.1. Meteorological Data.* We acquired location-specific and time-resolved mixing heights and wind speeds for the years 2007−2009 from NASA's Modern-Era Retrospective Analysis for Research and Applications (MERRA).[31] MERRA uses the Goddard Earth Observing System (GEOS) atmospheric model to assimilate historical meteorological and climatological observations into a global data set with high spatiotemporal resolution (1/2° longitude × 2/3° latitude × 1 h; in the middle latitudes, these values correspond to a spatial resolution of ∼56 × 74 km). Each city in our data set was matched to the nearest MERRA grid point. The median distance between the centroid of each city's urbanized land area and the corresponding MERRA grid point was 23 km (10% trimmed range 10−34 km).

MERRA data provide the wind speed at a standard 10 m reference height. To obtain the mixing-height-averaged wind speed, we employed a truncated power-law relationship for wind speed versus height (see the Supporting Information).[13,29] We used literature-recommended values for the vertical interpolation of wind speed as default input parameters and considered alternate values in sensitivity analyses (see the Supporting Information).[29,32,33]

2.3.2. Breathing Rate. Volumetric breathing rates for populations follow diurnal patterns, owing to variations in the levels of physical activity and in physiological processes (e.g., circadian rhythm).[34−36] Few data sets are available to characterize the temporal pattern of breathing rate for large urban populations. Here, we developed a diurnal profile using time-activity data from a large probability-based sample of the U.S. population[37] and activity-dependent inhalation rates (see the Supporting Information).[35,36] Relative to the time-integrated mean, the diurnal profile varies from 47% lower (03:00 to 04:00 h) to 33% higher (at 15:00 h) (see the Supporting Information). For base-case and sensitivity analyses, the time-integrated mean breathing rate was taken to be 14.5 m^3 $person^{-1}$ d^{-1}, consistent with long-term average inhalation rates recommended by the U.S. Environmental Protection Agency (USEPA).[35] This metabolically derived value is comparable to those used in other recent iF analyses (range 13−14.5 m^3 $person^{-1}$ d^{-1}),[8,14,24] and lower than the upper-bound breathing rate value of 20 m^3 $person^{-1}$ d^{-1} employed in some studies.[9,13] To test the sensitivity of the results to the inferred time pattern of population breathing, we considered four alternative patterns: constant, a sinusoidal daily cycle[34] (amplitude ± 25% of the mean), and two previously published profiles for the United States (Figure SI.4, Supporting Information).[11,38]

2.3.3. Data for Each Urban Area. We estimated intake fractions for the 3646 worldwide urban areas that had at least 100 000 inhabitants in the year 2000 utilizing a data set compiled by Angel et al.[39,40] The total population in this data set (2.0 billion) accounts for 71% of the total year 2000 global urban population and 32% of the global population.[40] The following information is available for each city: population, land area (A, km^2, derived from satellite data),[41] and location (latitude and longitude). In cases where a contiguous urbanized area spans several administrative units (e.g., for "conurbations" or "urban agglomerations"), this database generally provides a single population and land area estimate for the urban portion of the entire metropolitan region. To our knowledge, this database contains the most consistent and comprehensive global set of urban population and land area data available.[42] We idealize each city as occupying a square-plan urban footprint ($L = W = A^{0.5}$) and consider variations in the aspect ratio, $\alpha = L/W$, as a sensitivity parameter.

2.3.4. Emissions Profile. Since concentrations of primary nonreactive or first-order decaying pollutants scale linearly with emissions, intake fractions are independent of emission rates that are constant. However, because breathing rates and meteorology vary systematically, diurnal emission rate patterns can influence the intake fraction. For base-case analyses, we developed an "archetypal" diurnal emissions profile based on mobile source

emission inventories for Beijing, China,[43] Mexico City, Mexico,[13] and New Delhi, India[44] (see the Supporting Information). The sensitivity of the results to the choice of diurnal emissions profile was tested using the following alternatives: (a) time-invariant emissions, (b) individual diurnal profiles from each of the three above cities, and (c) emissions scaled to diurnal vehicle activity data (vehicle km h^{-1}) from the USEPA National Emissions Inventory (Figure SI.5, Supporting Information).[45] Each simulation utilized a single diurnal profile. (We did not account for weekday−weekend differences in the timing of emissions or breathing rates.)

2.4. Steady-State Intake Fraction. As a complement to the time-dependent numerical solution described above, we illustrate here an approximate analytical solution that aids in conceptual interpretation of the results. Substituting the steady-state solution for eq 2 into eq 1 yields the following relationship for the iF of a conserved species in a square-plan urban area:[6,10,11]

$$\text{iF} \approx \overline{Q}_i(P/\sqrt{A})(\overline{1/uH}) = \overline{Q}_i(\text{LPD})(\text{DR})^{-1}$$

$$\approx \frac{\text{population breathing rate}}{\text{urban ventilation rate}} \qquad (3)$$

This relationship can be decomposed into three parameter groups that provide insight into the key drivers of iF.[11] The first term, $\overline{Q}_i$, is the time-averaged per-capita mean breathing rate (m^3 s^{-1} $person^{-1}$). The second group, linear population density (LPD = $P/\sqrt{A}$, persons m^{-1}), is a property of a city's urban form that represents the mean population per unit length (in the windward direction) of urbanized land.[11,46] The final parameter group, normalized dilution rate (DR = $(\overline{1/uH})^{-1}$), characterizes atmospheric dilution (wind speed times mixing height, m^2 s^{-1}).[11] For each city, we compute DR as the long-term harmonic mean of the product of linearly interpolated hourly values of u and H. The ratio DR/LPD can be intuitively understood as an effective per-capita atmospheric dilution rate available for an urban area. The intraurban intake fraction is proportional to the ratio of the population breathing rate to this per-capita atmospheric dilution rate (iF $\approx \overline{Q}_i[\text{DR/LPD}]^{-1}$).

3. RESULTS AND DISCUSSION

3.1. Global and Regional Intake Fraction Summary. Table 1 presents summary metrics of population-weighted and unweighted distributions of iF values. Among all cities, the population-weighted mean intraurban iF for distributed ground-level emissions of conserved pollutants is 39 ppm (IQR = 14−52 ppm). Population-weighted results are computed by weighting each city's iF by its population (i.e., equal weight per person), whereas unweighted results treat each city as a distinct

Table 1. Global Summary of Intraurban Intake Fraction, Demographic Parameters, and Meteorology[a,b]

	intake fraction (ppm)		population (millions)		LPD (persons m^{-1})		DR (m^2 s^{-1})	
range of values	0.6−260		0.1−34		5.8−780		32−10000	
AM (ASD)	39 (36)	*17 (18)*	4.2 (6.4)	*0.55 (1.4)*	170 (150)	*59 (58)*	540 (460)	*520 (460)*
GM (GSD)	26 (2.5)	*12 (2.2)*	1.5 (4.7)	*0.28 (2.6)*	110 (2.5)	*45 (2.0)*	470 (1.6)	*450 (1.6)*
median	26	*12*	1.4	*0.21*	110	*41*	450	*430*
IQR	14−52	*7.3−20*	0.42−5	*0.13−0.43*	57−220	*28−67*	370−550	*360−530*
$P_{10} − P_{90}$	7.7−80	*4.7−34*	0.18−13	*0.11−1.1*	33−370	*20−110*	300−770	*300−750*

[a]Nonitalicized entries (left column under each column head) reflect population-weighted statistics; italicized entries (right column under each column head) are unweighted results. [b]Abbreviations: LPD, linear population density; DR, normalized dilution rate; AM, arithmetic mean; ASD, arithmetic standard deviation; GM, geometric mean; GSD, geometric standard deviation; IQR, interquartile range; P_{10} and P_{90}, 10th and 90th percentiles of distribution.

unit with equal weight.[11] Because iF is correlated with population, weighted metrics better reflect the distribution of iF over the global population of city inhabitants. For the remainder of this paper, we employ population-weighted metrics of iF unless stated otherwise. All reported results reflect the full numerical solution to the iF model as outlined in section 2.2.

Intake fraction varies over almost 3 orders of magnitude among all cities (full range 0.6−260 ppm, 10% trimmed range 7.7−80 ppm). The population-weighted distribution of iF conforms well to a log-normal form (geometric mean (GM) 26 ppm, geometric standard deviation (GSD) 2.5, Figure SI.6, Supporting Information). Respectively 530, 260, and 120 million people live in cities with iF values greater than 50, 75, and 100 ppm.

3.1.1. Reduced-Form Intake Fraction Model. Variation in iF among cities is predicted well by a parsimonious regression model using the following three-parameter fit:

$$iF = (74.0 \text{ ppm})(LPD)^{0.980}(DR)^{-0.876}A^{-0.0497} \qquad (4)$$

where units on the parameters are as specified in section 2.4. This regression can be used with reasonable accuracy to rapidly estimate iF for any city in the global data set ($r^2 = 0.99$, root-mean-square prediction error 9%). In addition, the reduced-form model provides a framework for understanding how variation in iF is governed by urban form and meteorology. Globally, LPD is more variable than DR (interquartile ranges are 57−220 persons m^{-1} for LPD and 370−550 m^2 s^{-1} for DR). Holding other variables constant, an IQR increase in linear population density results in a 3.8-fold increase in iF, while an IQR reduction in normalized dilution rate results in only a 42% increase in iF.

3.1.2. Patterns of Intake Fraction by City Size, World Region, and Country. Larger cities tend to have higher iF values (Figure 1). To illustrate, we divide the city data set into three population-based groupings of nearly equal total population: small cities with between 100 000 and 600 000 inhabitants (32% of the total city population), medium cities
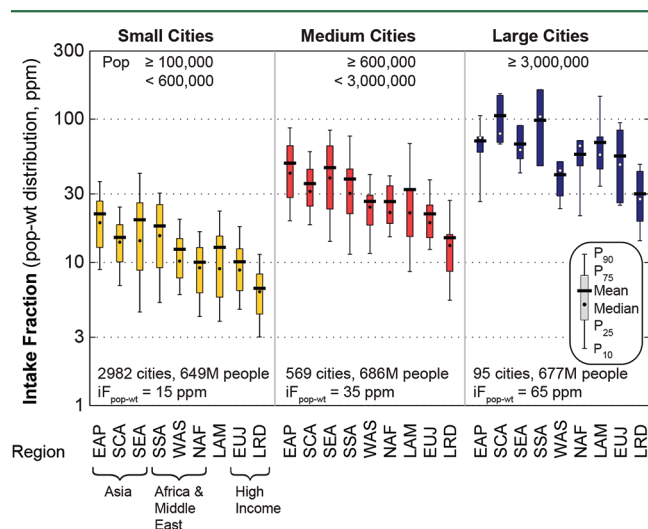

Figure 1. Population-weighted distribution of intraurban intake fraction by city size (small, medium, large) and region (labels on horizontal axis; see Table 2 and the map in Figure SI.7 (Supporting Information) for definitions of the abbreviations). For cities of similar size, iF is generally higher in Asia (e.g., EAP, SCA, and SEA) and lower in high-income regions (e.g., EUJ and LRD). See Table SI.3 (Supporting Information) for a tabulation of the results.

with 600 000 to 3 million inhabitants (34%), and large cities with >3 million inhabitants (34%). Population-weighted mean intraurban iF values for these three groupings are, respectively, 15, 35, and 65 ppm. Variation in iF by city size is principally attributable to the strong correlation between LPD and urban population. On average, each 1% increase in city population is associated with a 0.57% increase in LPD ($r^2 = 0.62$). Interestingly, LPD is much more variable among the three different city size groupings than is population density (mean LPD = 50, 130, and 310 persons m^{-1}, mean density = 110, 150, and 120 persons m^{-2}). The DR is uncorrelated with the population ($r^2 = 0.013$).

Intake fractions differ substantially among geographic regions (Table 2, Figures 1 and 2). Following Angel et al.,[39,40] we group the world into nine clusters that reflect varying land-use patterns (Figure SI.7, Supporting Information). Among these regions, mean intraurban iF varies by a factor of 2.7 (Table 2). Regions with especially high mean intraurban iF values include South and Central Asia (SCA; mean 55 ppm), Southeast Asia (SEA; 48 ppm), East Asia and the Pacific (EAP; 44 ppm), and sub-Saharan Africa (SSA; 43 ppm). By contrast, iF is comparatively low for land-rich developed countries (LRD; 20 ppm). Comparing Asia with North and Central America highlights regional properties of urban settlement (Figure 2). The Asian cities mapped in Figure 2 have a high mean intraurban iF (48 ppm) and a large total population (914 million, ∼45% of all global city inhabitants). Of all cities with intraurban iF ≥ 100 ppm (n = 24 cities), 75% (n = 18) are in Asia and 50% (n = 12) are in China.

Regional patterns of iF are independent of city size, such that similar trends in iF emerge within each of the small, medium, and large city groupings (Figure 1). As a result, iF values for smaller cities in some regions may be greater than those for more populous cities elsewhere. For example, the mean iF for small cities in EAP (22 ppm) is greater than that for medium cities in LRD (15 ppm).

Country-average intraurban iF varies by more than a factor of 3 among the 10 countries with the largest urban populations (Table 3; Table SI.9, Supporting Information). Mean intraurban iF values in Mexico (65 ppm), Indonesia (53 ppm), India (51 ppm), and China (44 ppm) are greater than in Australia (14 ppm), the United States (21 ppm), Germany (30 ppm), and Russia (32 ppm).

Regional variation in iF is attributable to urban form and meteorology (Table 2). For example, the high mean iF value in South and Central Asia (41% greater than the global mean) is attributable to high LPD (37% greater than the global mean) and weaker-than-average dilution (DR 9% below the global mean). Similarly, relatively low iF in land-rich developed countries (47% lower than the global mean) is explained by low LPD (36% lower than the global mean) and more favorable atmospheric dilution (DR 11% greater than the global mean). The range in LPD among the nine regions is roughly twice as large as the range for DR (Table 2). However, local patterns in wind speed and mixing height give rise to apparent "hotspots" where meteorology has a more pronounced role influencing iF. For example, DR is ∼30−60% lower than the global average in the Indo-Gangetic Plain (Pakistan, northern India, Bangladesh) and in heavily forested equatorial regions (Amazon and Congo River basins, parts of Indonesia). Globally, spatial variation in long-term DR depends more on the variation in wind speed than on the variation in mixing height.

3.1.3. Megacities. The air quality challenge of megacities (population >10 million) has received considerable attention.[47−55]

Table 2. Regional Summary of Intraurban Intake Fraction, Population Density, and Meteorology[a]

region		iF (ppm)	LPD (persons m⁻¹)	density (persons ha⁻¹)	DR (m² s⁻¹)	city population (millions)	N (cities)
SCA	South and Central Asia	55	230	160	490	290	539
SEA	Southeast Asia	48	170	120	520	110	196
EAP	East Asia and Pacific	44	180	220	480	460	891
SSA	sub-Saharan Africa	43	160	170	610	130	258
LAM	Latin America	41	170	87	610	260	403
NAF	North Africa	32	180	130	630	53	115
EUJ	Europe and Japan	30	140	59	530	400	796
WAS	Western Asia	26	120	91	550	90	157
LRD	land-rich developed	20	110	29	600	230	291

[a]Population-weighted arithmetic means for cities with populations ≥100 000. Total population 2.0 billion people (72% of the year 2000 urban population, 32% of the global population) in 3646 cities.

Table 3. Population-Weighted Mean Intraurban Intake Fraction for the 10 Countries with the Largest Population in Cities[a]

country	iF (ppm)	city population (millions)	country	iF (ppm)	city population (millions)
China	44	412	Mexico	65	58
United States	21	192	Germany	30	49
India	51	188	Indonesia	53	40
Brazil	33	88	South Korea	46	36
Japan	50	85	all 10 countries	41	1216
Russia	32	68	other 148 countries	35	796

[a]The cities considered are all urban areas with populations ≥100 000.

The 20 megacities in this data set account for ∼15% of the total city population (300 million people) and have a population-weighted mean iF of 83 ppm (IQR = 48−94 ppm, range 25−260 ppm). Four megacities have intake fractions that exceed 100 ppm: New Delhi, India; Kolkata, India; Dhaka, Bangladesh; and Mexico City, Mexico (Figure 2; Table SI.8, Supporting Information). Although the overall population density for megacities is nearly the same as the global mean for cities of all sizes (mean 125 persons ha⁻¹), the LPD in megacities is 2.5 times the global urban average (410 [megacities] versus 170 [global average], persons m⁻¹) owing to megacities' large spatial extent (mean area 2300 km²).

The total intraurban population intake ($E \times iF$) of emissions in megacities may be especially high. Megacities have been identified elsewhere as emissions hotspots.[48,50,52] High iF in megacities magnifies the exposure relevance of these emissions. For example, consider a hypothetical pollutant emitted on an equal per-capita basis everywhere. For that pollutant, a city's total intraurban intake would scale with the product of population and iF. Under such conditions, the world's 20 megacities would themselves account for 32% of the global intraurban intake or more than double the 15% of the global city population that they contain.

3.1.4. Time of Day and Seasonal Patterns in iF. Diurnal trends in atmospheric mixing and population breathing rate lead to variability in iF as a function of emissions timing. In general, iF is elevated for emissions that occur during periods of weak atmospheric dispersion (e.g., nighttime, Figure SI.8, Supporting Information). Considering all cities, the median iF for emissions at night (21:00 to 03:00 h) is 8.5 times greater (IQR = 5.1−11 times) than for emissions during the day (09:00 to 15:00 h). The strong role of atmospheric mixing in driving nighttime maxima in iF is highlighted when considering that our model accounts for higher-than-average population breath-

ing rates during daytime hours. Interestingly, diurnal cycles in mixing height are principally responsible for the temporal pattern in a city's short-term DR, in contrast to the observation above that regional variation in long-term DR is primarily attributable to between-city differences in mean wind speed.

Compared to diurnal variability, monthly differences in iF are less pronounced. The median ratio of maximum to minimum month-averaged iF among all cities is 2.3 (IQR = 1.8−2.9). On average, iF values in nontropical cities are 13 times greater (IQR = 9.1−15 times) during winter nights than summer days. Interannual variability in meteorology for the 3 years considered in this study (2007−2009) has a negligible (<1%) effect on global mean iF and also little effect on iF values for individual cities (10% trimmed range ∼±5%).

3.2. Validation and Comparison with Prior Research. Several previous studies have estimated iF values of urban vehicle emissions for individual cities, countries, or regions, principally in North America and Europe. For large groups of cities with diverse population sizes, prior estimates of population-weighted average iF values for vehicle emissions are in the range of ∼5−20 ppm,[9,11,22,56] with higher iF values reported for individual large cities (e.g., Mexico City, Hong Kong, Los Angeles).[12−14,23] The higher population-weighed mean iF result obtained here (39 ppm) is substantially attributable to the inclusion for the first time of many cities in Africa, Asia, and South America, which tend to have higher LPD than urban areas elsewhere (Table 2). Our core result—a global population-weighted mean intraurban iF of 39 ppm—is approximately consistent with the estimated "archetypal" iF by Humbert et al. (49 ppm, breathing-rate-adjusted) for ground-level emissions.[8]

Model results for individual cities and countries agree favorably with those of previous studies after adjustment for differences in breathing rate. Overall, agreement is stronger for groups of cities (e.g., national averages of cities) than for individual urban areas. For example, our estimate for population-weighted mean intraurban iF for the 243 U.S. cities with populations ≥100 000 (21 ppm) is similar to the estimate of Marshall et al. (2005) for U.S. Census "urban areas" (17 ppm, breathing-rate-adjusted).[11] Likewise, our estimate for metropolitan Los Angeles (43 ppm) is consistent with an empirically derived iF estimate for the South Coast Air Basin (38 ppm, breathing-rate-adjusted).[12] Our results for Mexico City and Hong Kong—two cities with notoriously complex terrains—each differ from prior empirical estimates by ∼50%, but in opposite directions. For Mexico City, our estimate (140 ppm) is ∼60% larger than that of Stevens et al. (87 ppm, breathing-rate-adjusted).[13] In contrast, our estimate for Hong Kong (110 ppm) is ∼40% lower than the value estimated by Luo et al.
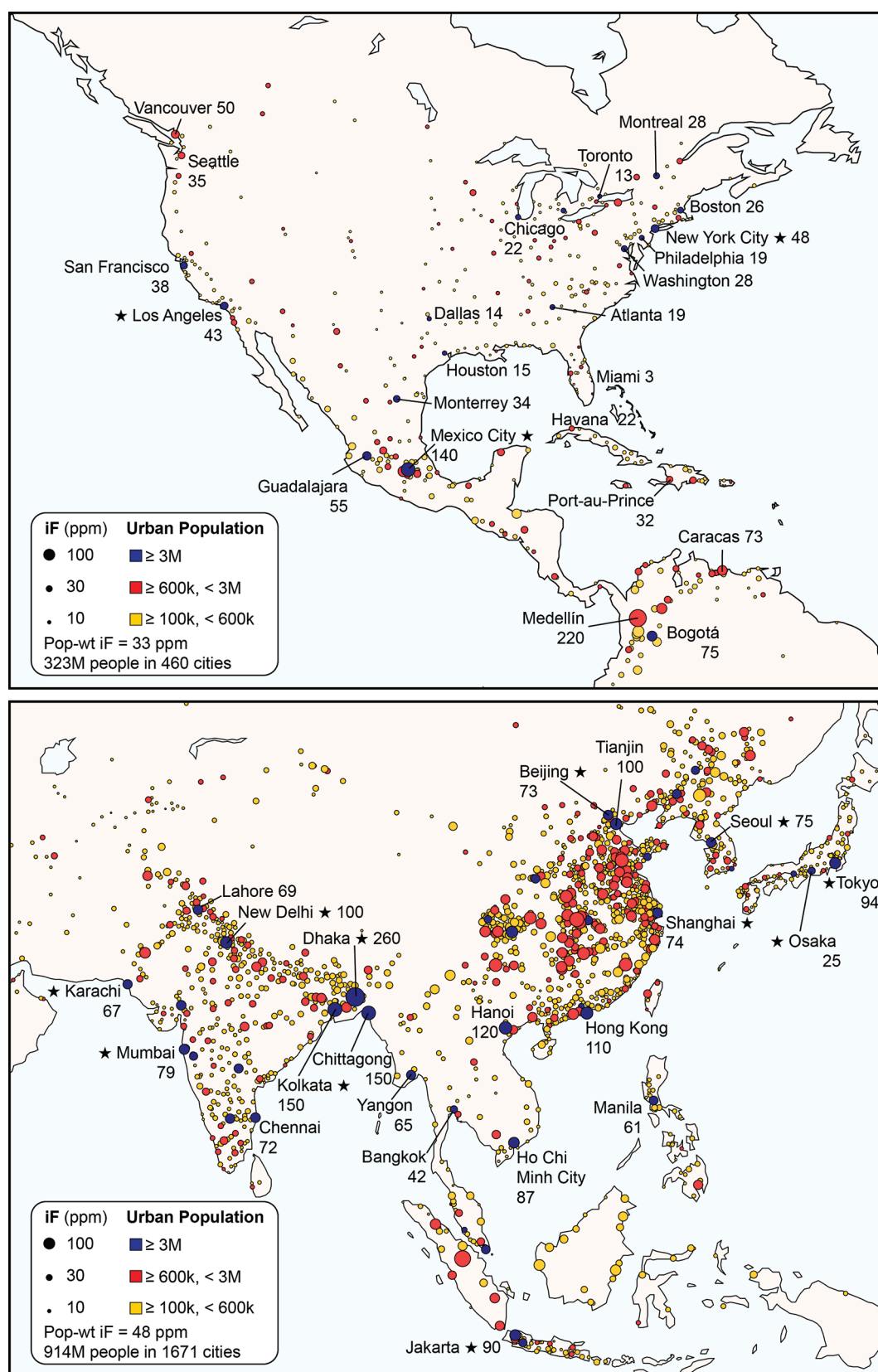
Figure 2. Map of intraurban intake fraction for cities in the Americas (upper panel) and Asia (lower panel). Values of iF are denoted by symbol area. City colors correspond with Figure 1 and indicate population size bins. Intake fractions for selected cities are labeled. Stars designate megacities (population >10 million, 11 on Asia map, 3 on Americas map). The same scale applies to both maps. The Supporting Information provides maps for other continents.

(190 ppm, breathing-rate-adjusted).[14] We obtain more closely comparable iF estimates for these two cities (to within ∼±30%)

after harmonizing demographic input parameters, which can vary substantially among studies of megacities.[57] Overall, the

results are consistent with an expectation of less than a factor of two uncertainty in iF values for individual cities estimated using the single-compartment Eulerian model.

While beyond the scope of the present study, further empirical validation of urban iF results is warranted. For example, emissions and concentration data for opportunistic tracer pollutants have already been used to develop semi-empirical iF estimates in several worldwide urban areas; for motor vehicles, example tracer species include CO, benzene, and diesel $PM_{2.5}$.[12−14,23,24] Recent improvements in global emissions data sets and satellite remote sensing techniques may permit more extensive use of empirical methods for assessing intake fractions in the future as a complement to the modeling approach employed here.

3.3. Sensitivity Analysis and Limitations. We tested the sensitivity of our results to many assumptions and modeling decisions that were necessary to assess iF at a global scale. On the basis of comparison with previous work (section 3.2), we estimate that the overall uncertainty for the aggregated (many-city) iF estimates is ∼30%.

Base-case analyses evaluate iF for nonreactive primary pollutants ($k = 0$). For nonconserved pollutants that follow first-order decay (half-lives 100 and 10 h), the mean iF is, respectively, only 0.8% and 7.2% lower than for conserved, nonreactive pollutants. The effect of decay was somewhat larger for large cities (11% for a 10 h half-life) owing to the longer residence time of air in cities with a greater length scale. Nevertheless, we found similar global patterns of iF with respect to region and city size for all three pollutant classes considered. Since the half-life for many health-relevant primary pollutants in urban air is larger than 10 h,[30] these findings imply that iF values for nonreactive pollutants may be reasonably applied to many toxic emissions to urban outdoor air. However, the iF values reported here may not be applicable to pollutants formed via secondary processes. For example, prior research indicates that intraurban iF may be 1−2 orders of magnitude lower for secondary $PM_{2.5}$ attributable to urban precursor emissions than for primary $PM_{2.5}$.[8−10]

In general, the results are relatively insensitive to most of the assumptions that we made in preprocessing meteorological parameters (section 2.3.1; Table SI.4, Supporting Information). However, the results for time-averaged iF are moderately sensitive to assumptions that relate to transient conditions of poor atmospheric mixing (e.g., during nights with low wind speeds). For example, the global mean iF is 35% lower in a sensitivity scenario under which the urban mixing height is constrained to be at least 100 m at all times. Since dispersion is generally weak at nights, alternative scenarios with higher emissions (E) or breathing rate (Q) at night result in higher iF values. The mean iF varies by 5−15% under a range of plausible assumptions about the diurnal pattern of E and Q (Table SI.5, Supporting Information). Refined model inputs for nighttime conditions may improve the accuracy of iF estimates in future studies.

An important modeling simplification relates to the aspect ratio, α, the ratio of an urban area's windward to crosswind dimensions (section 2.3.3). In the default modeling case, we assume square-plan layout ($\alpha = 1$), as α is not readily estimated for cities in this data set. In general, iF is expected to increase for situations where $\alpha > 1$ (less ventilation per unit land area), with the opposite true for $\alpha < 1$. The intake fraction for individual cities increased (decreased) by ∼30% for sensitivity cases in which $\alpha = 2$ ($\alpha = 0.5$). More detailed information on α

may therefore improve the precision of iF estimates for individual cities.

The modeling approach employed here has limitations. The one-compartment model does not account for within-urban variation in exposure concentrations or for the effects of micro-environments. To the extent that exposures disproportionately occur in near-source regions (e.g., in vehicles on roads), iF may be systematically underestimated by the model. Conversely, the model may overestimate iF when outdoor-attributable indoor exposure concentrations are attenuated from ambient levels, as is the case for $PM_{2.5}$ encountered in buildings.[58] Considering limiting cases (see the Supporting Information), the effect of microenvironmental exposure modification is estimated to account for <30% absolute uncertainty, roughly consistent with estimates elsewhere.[12,38]

A further limitation is that the model only assesses intraurban iF, the fraction of a city's emissions that are inhaled by that city's own inhabitants. The results exclude additional intake that may occur in other urban or rural areas downwind of the source city and therefore may be considered a lower-bound estimate of total iF. Limited prior research suggests that intraurban iF for ground-level emissions may reasonably approximate the total iF in many circumstances.[20,59] Nevertheless, the difference between intraurban and total iF may be important in certain cases, such as for emissions in a small urban area that is located upwind and near large urban areas.

Since inhalation intake is an incomplete indicator of health risk, additional analyses are required to interpret iF results more explicitly in terms of health effects. In general, a metric of "intake-based toxicity" (IBT; sample units: mortality per mass intake) can be combined with iF to yield estimates of health effect per unit emission.[19,60] IBT may vary among populations. For example, similar reductions in intake may yield differential health benefits among populations with differing baseline exposure levels, susceptibilities, and underlying disease burdens.[61]

3.4. Implications for Policy. Given constrained resources for environmental protection, air quality policies may seek to maximize the environmental health benefit achieved per unit cost expended. Intake fraction lends insight into one dimension of this calculus: the population intake benefit associated with a given quantity of emissions reduction. In concert with other information routinely used in air quality management and health risk assessment (e.g., source strengths, cost-of-control curves, pollutant toxicity data), it may be advantageous to prioritize emissions reductions for sources with high iF.[10,62−64] The global average iF for urban vehicle emissions (39 ppm) is substantially greater than previous estimates of iF for central electric power stations located in California, U.S. (∼1 ppm),[20] or China (∼10 ppm),[21] reinforcing the relative importance of vehicle emissions control. Comparing among regions, our results suggest that mitigating or avoiding increases in urban vehicle emissions in countries with high iF (e.g., India, China, and Indonesia) may yield relatively high exposure-reduction benefits per unit of emissions reduction. Moreover, as vehicle fleets in these countries tend to be high emitting and rapidly growing, the marginal costs of emissions abatement may be favorable. The exposure benefits of emissions control in megacities also appear particularly strong. Intake fraction results by season and time of day suggest that emissions control measures for ground-level sources with high emissions at night (e.g., trucking)[65] or during the winter (e.g., solid-fuel combustion for heat)[24,56] may yield relatively high exposure benefits per unit mitigation.

ASSOCIATED CONTENT

S **Supporting Information**

Additional description of the methodology and results, including figures and tables of urban- and national-level iF data. This material is available free of charge via the Internet at http://pubs.acs.org/

AUTHOR INFORMATION

Corresponding Author
*E-mail: julian@umn.edu; phone: (612) 625-2397; fax: (612) 626-7750.

Notes
The funding agencies neither reject nor endorse the conclusions and views expressed herein.
The authors declare no competing financial interest.

ACKNOWLEDGMENTS

REFERENCES

(1) Pope, C. A.; Dockery, D. W. Health effects of fine particulate air pollution: Lines that connect. *J. Air Waste Manage. Assoc.* **2006**, *56*, 709−742.

(2) Pope, C. A.; Ezzati, M.; Dockery, D. W. Fine-particulate air pollution and life expectancy in the United States. *N. Engl. J. Med.* **2009**, *360*, 376−386.

(3) Kampa, M.; Castanas, E. Human health effects of air pollution. *Environ. Pollut.* **2008**, *151*, 362−367.

(4) *Global Health Risks: Mortality and Burden of Disease Attributable to Selected Major Risks*; World Health Organization: Geneva, Switzerland, 2009; http://www.who.int/healthinfo/global_burden_disease/GlobalHealthRisks_report_full.pdf. Accessed: Feb 24, 2012.

(5) Bennett, D. H.; McKone, T. E.; Evans, J. S.; Nazaroff, W. W.; Margni, M. D.; Jolliet, O.; Smith, K. R. Defining intake fraction. *Environ. Sci. Technol.* **2002**, *36*, 206A−211A.

(6) Lai, A. C. K.; Thatcher, T. L.; Nazaroff, W. W. Inhalation transfer factors for air pollution health risk assessment. *J. Air Waste Manage. Assoc.* **2000**, *50*, 1688−1699.

(7) Rosenbaum, R. K.; Margni, M.; Jolliet, O. A flexible matrix algebra framework for the multimedia multipathway modeling of emission to impacts. *Environ. Int.* **2007**, *33*, 624−634.

(8) Humbert, S.; Marshall, J. D.; Shaked, S.; Spadaro, J. V.; Nishioka, Y.; Preiss, P.; McKone, T. E.; Horvath, A.; Jolliet, O. Intake fraction for particulate matter: Recommendations for life cycle impact assessment. *Environ. Sci. Technol.* **2011**, *45*, 4808−4816.

(9) Greco, S. L.; Wilson, A. M.; Spengler, J. D.; Levy, J. I. Spatial patterns of mobile source particulate matter emissions-to-exposure relationships across the United States. *Atmos. Environ.* **2007**, *41*, 1011−1025.

(10) Evans, J. S.; Wolff, S. K.; Phonboon, K.; Levy, J. I.; Smith, K. R. Exposure efficiency: An idea whose time has come? *Chemosphere* **2002**, *49*, 1075−1091.

(11) Marshall, J. D.; Teoh, S. K.; Nazaroff, W. W. Intake fraction of nonreactive vehicle emissions in US urban areas. *Atmos. Environ.* **2005**, *39*, 1363−1371.

(12) Marshall, J. D.; Riley, W. J.; McKone, T. E.; Nazaroff, W. W. Intake fraction of primary pollutants: Motor vehicle emissions in the South Coast Air Basin. *Atmos. Environ.* **2003**, *37*, 3455−3468.

(13) Stevens, G.; de Foy, B.; West, J. J.; Levy, J. I. Developing intake fraction estimates with limited data: Comparison of methods in Mexico City. *Atmos. Environ.* **2007**, *41*, 3672−3683.

(14) Luo, Z.; Li, Y.; Nazaroff, W. W. Intake fraction of nonreactive motor vehicle exhaust in Hong Kong. *Atmos. Environ.* **2010**, *44*, 1913−1918.

(15) Baidya, S.; Borken-Kleefeld, J. Atmospheric emissions from road transportation in India. *Energy Policy* **2009**, *37*, 3812−3822.

(16) Pucher, J.; Korattyswaropam, N.; Mittal, N.; Ittyerah, N. Urban transport crisis in India. *Transp. Policy* **2005**, *12*, 185−198.

(17) Chang, D.; Song, Y.; Liu, B. Visibility trends in six megacities in China 1973−2007. *Atmos. Res.* **2009**, *94*, 161−167.

(18) He, K.; Huo, H.; Zhang, Q.; He, D.; An, F.; Wang, M.; Walsh, M. P. Oil consumption and CO_2 emissions in China's road transport: Current status, future trends, and policy implications. *Energy Policy* **2005**, *33*, 1499−1507.

(19) Ji, S.; Cherry, C. R.; Bechle, M. J.; Wu, Y.; Marshall, J. D. Electric vehicles in China: Emissions and health impacts. *Environ. Sci. Technol.* **2012**, *46*, 2018−2024.

(20) Heath, G. A.; Granvold, P. W.; Hoats, A. S.; Nazaroff, W. W. Intake fraction assessment of the air pollutant exposure implications of a shift toward distributed electricity generation. *Atmos. Environ.* **2006**, *40*, 7164−7177.

(21) Zhou, Y.; Levy, J. I.; Evans, J. S.; Hammitt, J. K. The influence of geographic location on population exposure to emissions from power plants throughout China. *Environ. Int.* **2006**, *32*, 365−373.

(22) Tainio, M.; Sofiev, M.; Hujo, M.; Tuomisto, J. T.; Loh, M.; Jantunen, M. J.; Karppinen, A.; Kangas, L.; Karvosenoja, N.; Kupiainen, K.; Porvari, P.; Kukkonen, J. Evaluation of the European population intake fractions for European and Finnish anthropogenic primary fine particulate matter emissions. *Atmos. Environ.* **2009**, *43*, 3052−3059.

(23) Loh, M. M.; Soares, J.; Karppinen, A.; Kukkonen, J.; Kangas, L.; Riikonen, K.; Kousa, A.; Asikainen, A.; Jantunen, M. J. Intake fraction distributions for benzene from vehicles in the Helsinki metropolitan area. *Atmos. Environ.* **2009**, *43*, 301−310.

(24) Ries, F. J.; Marshall, J. D.; Brauer, M. Intake fraction of urban wood smoke. *Environ. Sci. Technol.* **2009**, *43*, 4701−4706.

(25) Marshall, J. D.; Behrentz, E. Vehicle self-pollution intake fraction: Children's exposure to school bus emissions. *Environ. Sci. Technol.* **2005**, *39*, 2559−2563.

(26) Stevens, G.; Wilson, A.; Hammitt, J. K. A benefit-cost analysis of retrofitting diesel vehicles with particulate filters in the Mexico City metropolitan area. *Risk Anal.* **2005**, *25*, 883−899.

(27) Bennett, D. H.; Margni, M. D.; McKone, T. E.; Jolliet, O. Intake fraction for multimedia pollutants: A tool for life cycle analysis and comparative risk assessment. *Risk Anal.* **2002**, *22*, 905−918.

(28) Cahill, T. M.; Mackay, D. Complexity in multimedia mass balance models: When are simple models adequate and when are more complex models necessary? *Environ. Toxicol. Chem.* **2003**, *22*, 1404−1412.

(29) Seinfeld, J. H.; Pandis, S. N. *Atmospheric Chemistry and Physics: From Air Pollution to Climate Change*, 2nd ed.; Wiley-Interscience: Hoboken, NJ, 2006.

(30) Atkinson, R. Atmospheric chemistry of VOCs and NO_x. *Atmos. Environ.* **2000**, *34*, 2063−2101.

(31) Rienecker, M. M.; Suarez, M. J.; Gelaro, R.; Todling, R.; Bacmeister, J.; Liu, E.; Bosilovich, M. G.; Schubert, S. D.; Takacs, L.; Kim, G.-K.; Bloom, S.; Chen, J.; Collins, D.; Conaty, A.; da Silva, A.; Gu, W.; Joiner, J.; Koster, R. D.; Lucchesi, R.; Molod, A.; Owens, T.; Pawson, S.; Pegion, P.; Redder, C. R.; Reichle, R.; Robertson, F. R.; Ruddick, A. G.; Sienkiewicz, M.; Woollen, J. MERRA: NASA's Modern-Era Retrospective Analysis for Research and Applications. *J. Clim.* **2011**, *24*, 3624−3648.

(32) Hanna, S. R.; Briggs, G. A.; Hosker, R. P., Jr. *Handbook on Atmospheric Diffusion*; DOE/TIC-112233; Office of Energy and Research, U.S. Department of Energy: Washington, DC, 1982; http://www.orau.org/ptp/PTP Library/library/Subject/Meteorology/handbook on atmospheric diffusion.pdf. Accessed: Feb 24, 2012.

(33) Irwin, J. S. A theoretical variation of the wind profile power-law exponent as a function of surface roughness and stability. *Atmos. Environ.* **1979**, *13*, 191−194.

(34) Stephenson, R.; Mohan, R. M.; Duffin, J.; Jarsky, T. M. Circadian rhythms in the chemoreflex control of breathing. *Am. J. Physiol.: Regul., Integr. Comp. Physiol.* **2000**, *278*, R282−R286.

(35) *Exposure Factors Handbook: 2009 Update (External Review Draft)*; EPA/600/R-09/052A; U.S. Environmental Protection Agency: Washington, DC, 2009; http://cfpub.epa.gov/ncea/cfm/recordisplay.cfm?deid=209866. Accessed: Feb 24, 2012.

(36) *Metabolically Derived Human Ventilation Rates: A Revised Approach Based upon Oxygen Consumption Rates*; EPA/600/R-06/129F; U.S. Environmental Protection Agency, National Center for Environmental Assessment: Washington, DC, 2009; http://cfpub.epa.gov/ncea/cfm/recordisplay.cfm?deid=202543. Accessed: Feb 24, 2012.

(37) Klepeis, N. E.; Nelson, W. C.; Ott, W. R.; Robinson, J. P.; Tsang, A. M.; Switzer, P.; Behar, J. V.; Hern, S. C.; Engelmann, W. H. The National Human Activity Pattern Survey (NHAPS): A resource for assessing exposure to environmental pollutants. *J. Exposure Anal. Environ. Epidemiol.* **2001**, *11*, 231−252.

(38) Marshall, J. D.; Granvold, P. W.; Hoats, A. S.; McKone, T. E.; Deakin, E.; Nazaroff, W. W. Inhalation intake of ambient air pollution in California's South Coast Air Basin. *Atmos. Environ.* **2006**, *40*, 4381−4392.

(39) Angel, S.; Parent, J.; Civco, D.; Blei, A.; Potere, D. *A Planet of Cities: Urban Land Cover Estimates and Projections for All Countries, 2000−2050*; WP10SA3; Lincoln Institute of Land Policy: Cambridge, MA, 2010; http://www.lincolninst.edu/pubs/1861_A-Planet-of-Cities. Accessed: Feb 24, 2012.

(40) Angel, S.; Parent, J.; Civco, D. L.; Blei, A.; Potere, D. The dimensions of global urban expansion: Estimates and projections for all countries, 2000−2050. *Prog. Plann.* **2011**, *75*, 53−107.

(41) Schneider, A.; Friedl, M. A.; Potere, D. A new map of global urban extent from MODIS satellite data. *Environ. Res. Lett.* **2009**, *4*, 044003.

(42) Potere, D.; Schneider, A.; Angel, S.; Civco, D. L. Mapping urban areas on a global scale: Which of the eight maps now available is more accurate? *Int. J. Remote Sens.* **2009**, *30*, 6531−6558.

(43) Huo, H.; Zhang, Q.; He, K.; Wang, Q.; Yao, Z.; Streets, D. G. High-resolution vehicular emission inventory using a link-based method: A case study of light-duty vehicles in Beijing. *Environ. Sci. Technol.* **2009**, *43*, 2394−2399.

(44) Guttikunda, S. K. Diurnal profiles for Delhi emissions inventory, personal communication, June 8, 2011.

(45) *The National Emissions Inventory*; U.S. Environmental Protection Agency: Washington, DC, 2011; http://www.epa.gov/ttn/chief/net/2008inventory.html. Accessed: Feb 24, 2012.

(46) Marshall, J. D. Urban land area and population growth: A new scaling relationship for metropolitan expansion. *Urban Stud.* **2007**, *44*, 1889−1904.

(47) Mage, D.; Ozolins, G.; Peterson, P.; Webster, A.; Orthofer, R.; Vandeweerd, V.; Gwynne, M. Urban air pollution in megacities of the world. *Atmos. Environ.* **1996**, *30*, 681−686.

(48) Guttikunda, S. K.; Tang, Y.; Carmichael, G. R.; Kurata, G.; Pan, L.; Streets, D. G.; Woo, J.-H.; Thongboonchoo, N.; Fried, A. Impacts of Asian megacity emissions on regional air quality during spring 2001. *J. Geophys. Res.* **2005**, *110*, D20301.

(49) Gurjar, B. R.; Butler, T. M.; Lawrence, M. G.; Lelieveld, J. Evaluation of emissions and air quality in megacities. *Atmos. Environ.* **2008**, *42*, 1593−1606.

(50) Butler, T. M.; Lawrence, M. G.; Gurjar, B. R.; van Aardenne, J.; Schultz, M.; Lelieveld, J. The representation of emissions from megacities in global emission inventories. *Atmos. Environ.* **2008**, *42*, 703−719.

(51) Gurjar, B. R.; Lelieveld, J. New directions: Megacities and global change. *Atmos. Environ.* **2005**, *39*, 391−393.

(52) Parrish, D. D.; Zhu, T. Clean air for megacities. *Science* **2009**, *326*, 674−675.

(53) Molina, M. J.; Molina, L. T. Megacities and atmospheric pollution. *J. Air Waste Manage. Assoc.* **2004**, *54*, 644−680.

(54) Wang, H.; Fu, L.; Zhou, Y.; Du, X.; Ge, W. Trends in vehicular emissions in China's mega cities from 1995 to 2005. *Environ. Pollut.* **2010**, *158*, 394−400.

(55) Chan, C. K.; Yao, X. Air pollution in mega cities in China. *Atmos. Environ.* **2008**, *42*, 1−42.

(56) Taimisto, P.; Tainio, M.; Karvosenoja, N.; Kupiainen, K.; Porvari, P.; Karppinen, A.; Kangas, L.; Kukkonen, J.; Tuomisto, J. Evaluation of intake fractions for different subpopulations due to primary fine particulate matter ($PM_{2.5}$) emitted from domestic wood combustion and traffic in Finland. *Air Qual. Atmos. Health* **2011**, *4*, 199−209.

(57) Forstall, R. L.; Greene, R. P.; Pick, J. B. Which are the largest? Why lists of major urban areas vary so greatly. *Tijdschr. Econ. Soc. Geogr.* **2009**, *100*, 277−297.

(58) Riley, W. J.; McKone, T. E.; Lai, A. C. K.; Nazaroff, W. W. Indoor particulate matter of outdoor origin: Importance of size-dependent removal mechanisms. *Environ. Sci. Technol.* **2002**, *36*, 200−207.

(59) Greco, S. L.; Wilson, A. M.; Hanna, S. R.; Levy, J. I. Factors influencing mobile source particulate matter emissions-to-exposure relationships in the Boston urban area. *Environ. Sci. Technol.* **2007**, *41*, 7675−7682.

(60) Marshall, J. D.; Nazaroff, W. W. Risk assessment of diesel-fired back-up electric generators operating in California, 2002; Appendix 4-2. http://z.umn.edu/dieselBUG. Accessed: Feb 24, 2012.

(61) Levy, J. I.; Greco, S. L.; Melly, S. J.; Mukhi, N. Evaluating efficiency-equality tradeoffs for mobile source control strategies in an urban area. *Risk Anal.* **2009**, *29*, 34−47.

(62) Roumasset, J. A.; Smith, K. R. Exposure trading: An approach to more efficient air pollution control. *J. Environ. Econ. Manage.* **1990**, *18*, 276−291.

(63) Smith, K. R. Fuel combustion, air pollution exposure, and health: The situation in developing countries. *Annu. Rev. Energy Environ.* **1993**, *18*, 529−566.

(64) Nazaroff, W. W. New directions: It's time to put the human receptor into air pollution control policy. *Atmos. Environ.* **2008**, *42*, 6565−6566.

(65) Sathaye, N.; Harley, R.; Madanat, S. Unintended environmental impacts of nighttime freight logistics activities. *Transp. Res. A* **2010**, *44*, 642−659.